

Real-time monitoring of internal temperature, flow rate and pressure in the high-temperature PEMFC stack using flexible integrated micro sensor

*Chi-Yuan Lee¹⁾, Fang-Bor Weng²⁾, Yen-Ting Huang³⁾, Yen-Pu Huang⁴⁾, Yen-Ting Cheng⁵⁾ and Chih-Kai Cheng⁶⁾

1), 2), 3), 4), 5), 6) Department of Mechanical Engineering, Yuan Ze Fuel Cell Center, Yuan Ze University, Taoyuan, Taiwan

¹⁾ cylee@saturn.yzu.edu.tw

ABSTRACT

During the chemical reaction process of high-temperature proton exchange membrane fuel cell (HT-PEMFC) stack, the non-uniformity of internal local temperature, flow rate and pressure would result in poor membrane durability, fuel distribution non-uniformity and adverse impact on the fuel cell stack performance and service life.

This study applies the micro-electro-mechanical systems (MEMS) technology to develop flexible integrated (temperature, flow rate and pressure) micro sensor resistant to the high-temperature electrochemical environment. Appropriate materials and processing parameters are selected to protect the integrated micro sensor from failure or damage in long term test. The internal local temperature, flow rate and pressure are monitored in real time. The proposed design has advantages of three sensing functions, compactness, acid corrosion resistance, good temperature tolerance, short response time, *in-situ* measurement and applicability to any position.

1. INTRODUCTION

The high temperature proton exchange membrane fuel cell stack (HT-PEMFC stack) is characterized by portable application, high energy conversion efficiency, no electrolyte loss, easy assembly and production and long operation life (Janssen 2013). In the past decade, research teams around the world have paid particular attention to HT-PEMFC stack (120~200°C) (Zhang 2006, Li 2009 and Chandan 2013).

At present, the development of Taiwan's fuel cell technology is mainly low temperature proton exchange membrane fuel cell stack (LT-PEMFC stack). The bottlenecks of low temperature fuel cell stack include (1) the anode catalyst has poor CO poisoning resistance in low temperature (<80°C) environment; (2) the perfluorosulfonic acid membrane has good ionic conductivity only in high humidity environment; (3) high cathodic reduction overpotential; (4) liquid water and heat removal management (Bose 2011), so that the bulk production schedule is delayed. Therefore, the latest international trend, such as U.S. DOE (Department of Energy), EU and Japan NEDO (New Energy Development Organization) develop towards high temperature fuel cell technology. However, the problems in the high temperature fuel cell stack, such as membrane material durability, catalyst corrosion, local flow, pressure and temperature nonuniformity inside the fuel cell stack, should be addressed to commercialize the fuel

cell stack. The real-time microscopic monitoring of local temperature, flow and pressure in the high temperature proton exchange membrane fuel cell stack is the topic of this study.

2. SENSING PRINCIPLE OF FLEXIBLE MICRO SENSOR

2.1 Sensing principle of micro temperature sensor

The design of micro temperature sensor is shown in Fig. 1. The sensing principle is that when the ambient temperature rises, as gold has positive temperature coefficient (PTC), the resistivity increases, this characteristic is resulted from the "temperature coefficient of resistance" (TCR) of conductor, defined as Eq. (1).

$$\alpha = \frac{1}{\rho_0} \frac{d\rho}{dT} \quad (1)$$

Eq. (1) shows the relationship between the temperature and resistance value of conductor is nonlinear, but if the resistance temperature detector is used in the linear range of resistance value of conductor, Eq. (1) can be reduced to Eq. (2).

$$R_t = R_r(1 + \alpha_1 \Delta T) \quad (2)$$

where the physical significance of temperature coefficient α_1 is the sensitivity of micro sensor, so Eq. (2) can be changed to Eq. (3).

$$\alpha_1 = \frac{R_t - R_r}{R_r(\Delta T)} \quad (3)$$

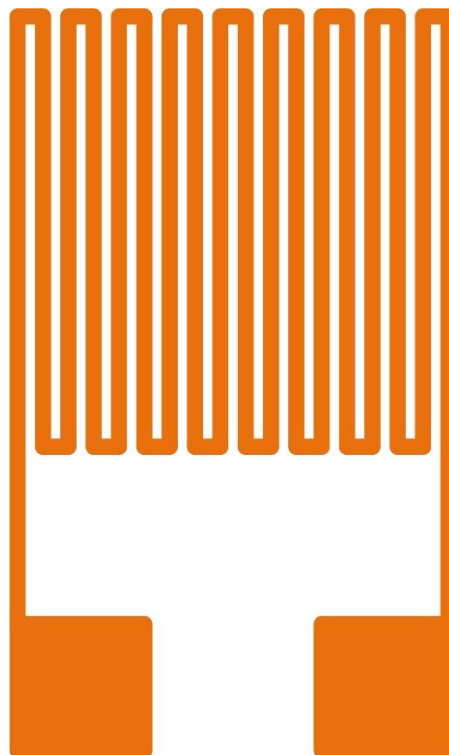


Fig. 1 Schematic diagram of design of micro temperature sensor

2.2 Sensing principle of micro flow sensor

The hot-wire micro flow sensor is designed according to the positive correlation between the thermal energy dissipation rate of hot wire and fluid flow. The sensing principle of hot-wire micro flow sensor is shown in Fig. 2.

According to King's law, the relationship between thermal energy dissipation rate and fluid flow rate is expressed as Eq. (4).

$$Q = I^2 \times R = I \times V = (A + B \times U^n) (T_s - T_o) \quad (4)$$

where Q is the electric power supplied from external power supply; U is the flow rate of fluid; n is the coefficient of correlation between heat Q and flow rate U , it is about 0.5 according to experiment; T_s is the temperature of hot wire; T_o is the temperature of inlet fluid; A is constant, the coefficient of heat transmitted by heater when the flow is fixed at zero; B is constant, the coefficient of heat from fluid and heater when the flow is not zero. Therefore, Eq. (4) can be changed to Eq. (5).

$$Q = (A + B \times U^{0.5}) \Delta T \quad (5)$$

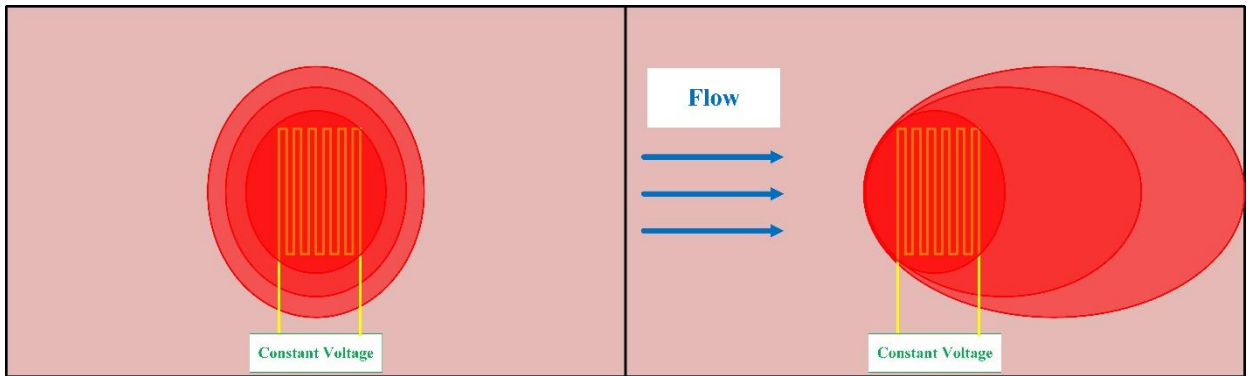


Fig. 2 Schematic diagram of sensing principle of micro flow sensor

2.3 Sensing principle of micro pressure sensor

The structure of capacitive micro pressure sensor is a nonconducting dielectric layer sandwiched in between two parallel electrodes. The capacitance value is calculated as Eq. (6).

$$\Delta C = \epsilon_r \epsilon_0 \frac{A}{\Delta d} \quad (6)$$

where ϵ_r is the dielectric constant of material, ϵ_0 is the constant 8.854×10^{-12} (F/m), A is the projection overlapping area of two parallel electrodes, Δd is the vertical distance variation between two parallel electrodes. According to Eq.(6), the dielectric constant and the projected area of two parallel electrodes only influence the initial capacitance value, the capacitance variation is influenced mainly by the variation of distance between two parallel electrodes.

If one electrode structure is deformable membrane, the dielectric layer is sensor of air or vacuum hollow structure, the capacitance is calculated as Eq. (7).

$$\Delta C = \iint \frac{\epsilon}{d - w(x, y)} dx dy \quad (7)$$

where $w(x,y)$ is the function of x-y deformation of membrane.

In order to enable the capacitive micro pressure sensor to present linear response, the sensitivity is increased and the process convenience is considered. The dielectric layer material of micro pressure sensor in this study is Fujifilm Durimide® PI 7320 with suitable stiffness, dielectric constant, elastic coefficient and process convenience. As the cavity between two parallel plate electrodes is replaced by polymers, the deformation of membrane electrode is average. In addition, the dielectric constant of PI 7320 is 3.2, in comparison to air dielectric constant 1. The micro pressure sensor has larger initial capacitance, and the capacitance variation is increased. Thus, the sensitivity is enhanced, facilitating micro pressure sensor correction and measurement (Chiang 2007). In order to locate the micro pressure sensor in the runner of high temperature fuel cell stack, the runner size is 1.1mm×1.1mm. If the micro pressure sensor is too large, the micro pressure sensor is likely to be pressed and destroyed or the measurement of micro pressure sensor is obstructed. Therefore, the capacitive sensing area is designed as 800μm×800μm, as shown in Fig. 3.

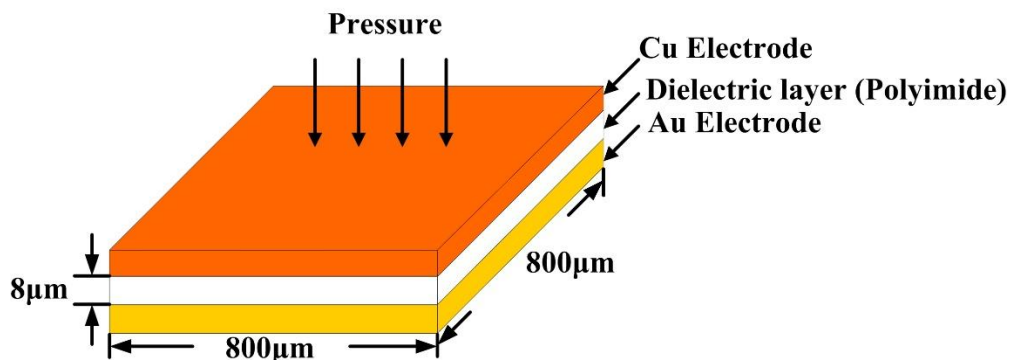


Fig. 3 Schematic diagram of design of capacitive micro pressure sensor

3. TEST RESULT OF CONSTANT CURRENT (5, 13, 20A) OUTPUT

In this experiment, the cell stack operating temperature is 160°C, the machine gives the anode and cathode fixed not humidified gases (anode H₂: 5slpm; cathode Air: 30slpm), and different loads are given constant current (5, 13, 20A), the output time is 60 minutes. The authentic information of local temperature, pressure and flow in the high temperature fuel cell stack is obtained by real-time continuous measurement of NI PXI 2575 data acquisition unit.

3.1 Local temperature distributions in different cells

Fig. 4 shows the local temperature in different cells. It is observed that the temperature increases gradually with the constant current (5, 13, 20A), as the higher the operating current is, the higher is the heat released from chemical reaction, and in the case of high current (20A), the thermal distribution nonuniformity becomes worse gradually. The temperature of Cell 10 is apparently lower than that of other cells, because the 3-in-1 micro sensor is close to the metal collector plate. The heat dissipation is fast, and the cathode terminal gas flow is high, it is room temperature when the gas is led in, so that the temperature of Cell 10 is lower. The temperature of Cell 5 is higher, it may be because Cell 5 is located in the center of high temperature cell

stack. The gases on both ends take the heat from the front end to the tail end. The internal chemical reaction is drastic in the case of high current (20A), and there is heat concentration, so that the temperature of Cell 5 is higher than other cells.

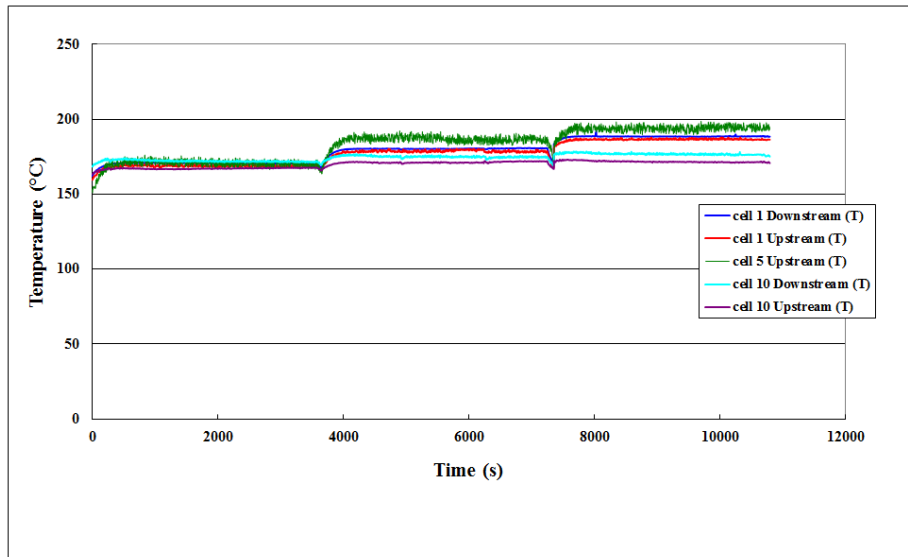


Fig. 4 Comparison diagram of local temperature and voltage in different cells

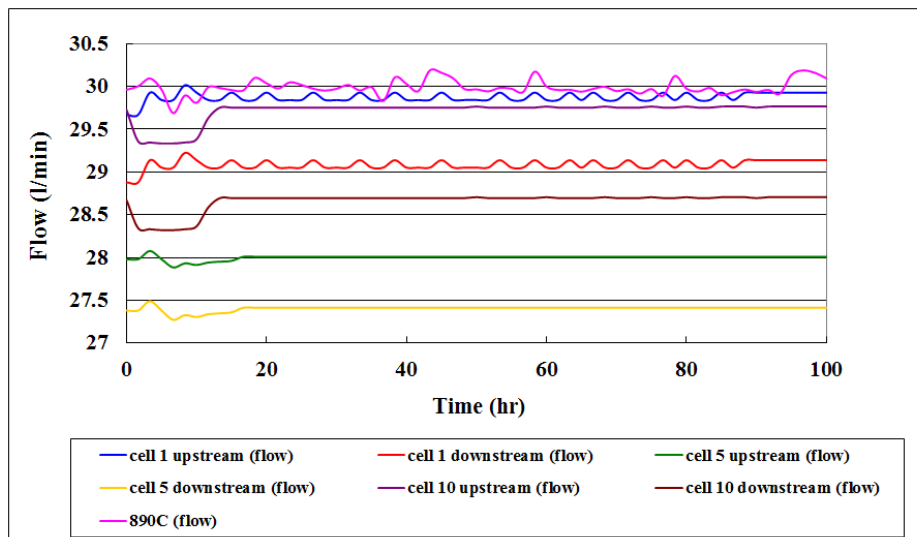


Fig. 5 Comparison diagram of local flow in different cells

3.2 Local flow rate distribution in different cells

Fig. 5 shows the local flow in different cells. It is observed that the upstream flow is higher than the downstream, and Cell 1 and Cell 10 are higher than Cell 5. Because the upstream flow of Cell 1 and Cell 10 is nearby the air inlet, the gas is sufficient. The downstream flow is lower, because the high temperature cell stack uses multiple snakelike runners in order to have better performance, the internal gas distribution is nonuniform, so that the downstream flow is lower. The flow of Cell 5 is lower than Cell 1 and Cell 10. This is because the Cell 5 is located in the center of high temperature cell

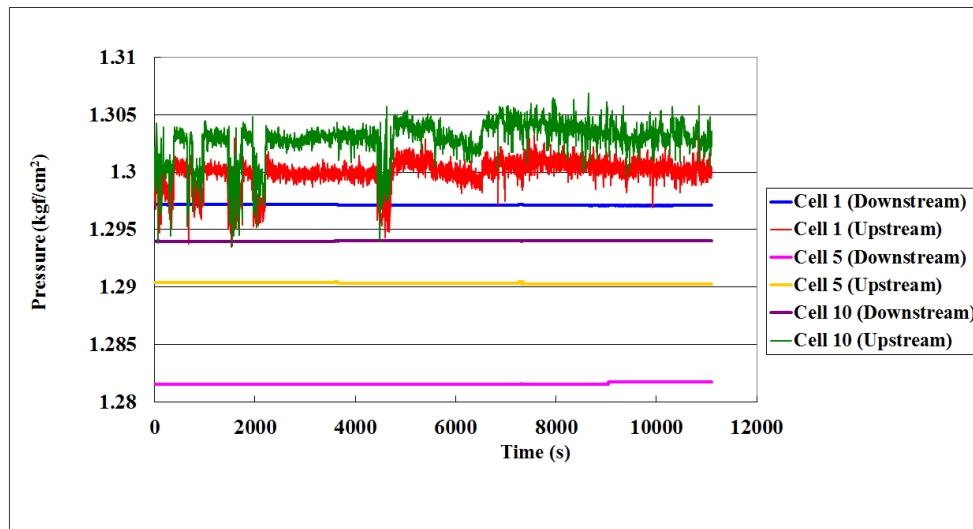


Fig. 6 Comparison diagram of local pressure in different cells

stack, and the gases on both ends are taken through single cells from the front end to the center. The flow is lost partially through each cell, so that the flow of Cell 5 is lower than other cells.

3.3 Local pressure distribution in different cells

Fig. 6 shows the local pressure in different cells. It is observed that the local pressure in the high temperature cell stack does not vary as the constant current (5, 13, 20A) increases. The downstream pressure is slightly higher than the upstream pressure. The average pressure in the high temperature cell stack is 1.25atm. The upstream pressure value of Cell 1 and Cell 10 fluctuates up and down. This is because the 3-in-1 micro sensor is close to the air inlets on both ends of cell stack, and the cathode terminal gas flow is high. Moreover, the upstream end pressure of Cell 1 and Cell 10 is unstable. It is stabilized at the downstream end. The upstream-downstream end pressure difference of Cell 5 is small, meaning the pressure in the high temperature cell stack is stable. It can be used to evaluate whether the design of internal flow field of high temperature cell stack is good or not.

4. CONCLUSIONS

This study used MEMS technology to develop a high temperature electrochemical environment resistant 3-in-1 (temperature, flow and pressure) micro sensor on 40 μ m thick stainless steel substrate. The protection layer is made of PI with better temperature tolerance. This high temperature electrochemical environment resistant 3-in-1 micro sensor has three functions. It is characterized by compactness, acid corrosion resistance, good temperature tolerance, quick response, real-time measurement and arbitrary location.

The local temperature, flow and pressure information inside the high temperature fuel cell stack are extracted successfully. The test result of operating temperature 160°C and constant current (5, 13, 20A) shows that the nonuniform temperature and flow distributions in the high temperature fuel cell stack.

5. ACKNOWLEDGEMENTS

This work was accomplished with much needed support and the authors would like to thank for the financial support by Ministry of Science and Technology of R.O.C. through the grant MOST 102-2221-E-155-033-MY3, 103-2622-E-155-006-CC2, 103-2622-E-155-018-CC2, 104-2623-E-155-004-ET and 104-2622-E-155-004. In addition, we would like to thank the YZU Fuel Cell Center and NENS Common Lab, for providing access to their research facilities.

REFERENCES

- Janssen, H., Supra, Lueke, J., Lehnert, L.W. and Stolten, D. (2013), "Development of HT-PEFC stacks in the kW range," *International Journal of Hydrogen Energy*, **38**, 4705-4713.
- Zhang, J., Xie, Z., Zhang, J., Tang, Y., Song, C., Navessin, T., Shi, Z., Song, D., Wang, H., Wilkinson, D.P., Liu, Z.S. and Holdcroft, S. (2006), "High temperature PEM fuel cells," *Journal of Power Sources*, **160**, 872-891.
- Li, Q., Jensen, J.O., Savinell, R.F. and Bjerruma, N.J. (2009), "High temperature proton exchange membranes based on polybenzimidazoles for fuel cells," *Progress in Polymer Science*, **34**, 449-477.
- Chandan, A., Hattenberger, M., El-Kharouf, A., Du, S.F., Dhir, A., Self, V., Pollet, B.G., Ingram, A. and Bujalski, W. (2013), "High temperature (HT) polymer electrolyte membrane fuel cells (PEMFC) - A review" *Journal of Power Sources*, **231**, 264-278.
- Bose, S., Kuila, T., Nguyen, T.X.H., Kim, N.H., Lau, K.T. and Lee, J.H. (2011), "Polymer membranes for high temperature proton exchange membrane fuel cell: recent advances and challenges," *Progress in Polymer Science*, **36**, 813-843.
- Chiang, C.C., Lin, C.K. and Ju, M.S. (2007), "An implantable capacitive pressure sensor for biomedical applications," *Sensors and Actuators A*, **134**, 382-388.